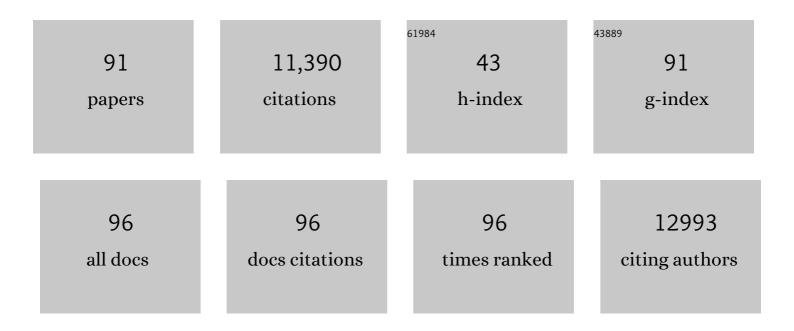
Hai Xiao

List of Publications by Year in descending order

Source: https://exaly.com/author-pdf/2107099/publications.pdf Version: 2024-02-01



HAL YIAO

#	Article	IF	CITATIONS
1	Direct observation of noble metal nanoparticles transforming to thermally stable single atoms. Nature Nanotechnology, 2018, 13, 856-861.	31.5	741
2	Copper atom-pair catalyst anchored on alloy nanowires for selective and efficient electrochemical reduction of CO2. Nature Chemistry, 2019, 11, 222-228.	13.6	571
3	Fe Isolated Single Atoms on S, N Codoped Carbon by Copolymer Pyrolysis Strategy for Highly Efficient Oxygen Reduction Reaction. Advanced Materials, 2018, 30, e1800588.	21.0	511
4	Accurate Band Gaps for Semiconductors from Density Functional Theory. Journal of Physical Chemistry Letters, 2011, 2, 212-217.	4.6	444
5	Schottky-Barrier-Free Contacts with Two-Dimensional Semiconductors by Surface-Engineered MXenes. Journal of the American Chemical Society, 2016, 138, 15853-15856.	13.7	444
6	Full atomistic reaction mechanism with kinetics for CO reduction on Cu(100) from ab initio molecular dynamics free-energy calculations at 298 K. Proceedings of the National Academy of Sciences of the United States of America, 2017, 114, 1795-1800.	7.1	414
7	Heterogeneous Fe3 single-cluster catalyst for ammonia synthesis via an associative mechanism. Nature Communications, 2018, 9, 1610.	12.8	409
8	Mechanistic Explanation of the pH Dependence and Onset Potentials for Hydrocarbon Products from Electrochemical Reduction of CO on Cu (111). Journal of the American Chemical Society, 2016, 138, 483-486.	13.7	381
9	Synergy between Fe and Ni in the optimal performance of (Ni,Fe)OOH catalysts for the oxygen evolution reaction. Proceedings of the National Academy of Sciences of the United States of America, 2018, 115, 5872-5877.	7.1	380
10	Subsurface oxide plays a critical role in CO ₂ activation by Cu(111) surfaces to form chemisorbed CO ₂ , the first step in reduction of CO ₂ . Proceedings of the National Academy of Sciences of the United States of America, 2017, 114, 6706-6711.	7.1	363
11	Theoretical Understandings of Graphene-based Metal Single-Atom Catalysts: Stability and Catalytic Performance. Chemical Reviews, 2020, 120, 12315-12341.	47.7	354
12	Breaking Long-Range Order in Iridium Oxide by Alkali Ion for Efficient Water Oxidation. Journal of the American Chemical Society, 2019, 141, 3014-3023.	13.7	337
13	Monolayer atomic crystal molecular superlattices. Nature, 2018, 555, 231-236.	27.8	323
14	Cu metal embedded in oxidized matrix catalyst to promote CO ₂ activation and CO dimerization for electrochemical reduction of CO ₂ . Proceedings of the National Academy of Sciences of the United States of America, 2017, 114, 6685-6688.	7.1	322
15	Atomistic Mechanisms Underlying Selectivities in C ₁ and C ₂ Products from Electrochemical Reduction of CO on Cu(111). Journal of the American Chemical Society, 2017, 139, 130-136.	13.7	320
16	Reaction Mechanisms for the Electrochemical Reduction of CO ₂ to CO and Formate on the Cu(100) Surface at 298 K from Quantum Mechanics Free Energy Calculations with Explicit Water. Journal of the American Chemical Society, 2016, 138, 13802-13805.	13.7	310
17	Constructing NiCo/Fe ₃ O ₄ Heteroparticles within MOF-74 for Efficient Oxygen Evolution Reactions. Journal of the American Chemical Society, 2018, 140, 15336-15341.	13.7	310
18	In Silico Discovery of New Dopants for Fe-Doped Ni Oxyhydroxide (Ni _{1–<i>x</i>} Fe _{<i>x</i>} OOH) Catalysts for Oxygen Evolution Reaction. Journal of the American Chemical Society, 2018, 140, 6745-6748.	13.7	274

#	Article	IF	CITATIONS
19	Three-dimensional open nano-netcage electrocatalysts for efficient pH-universal overall water splitting. Nature Communications, 2019, 10, 4875.	12.8	253
20	Surface Single-Cluster Catalyst for N ₂ -to-NH ₃ Thermal Conversion. Journal of the American Chemical Society, 2018, 140, 46-49.	13.7	233
21	Identification of the Electronic and Structural Dynamics of Catalytic Centers in Single-Fe-Atom Material. CheM, 2020, 6, 3440-3454.	11.7	231
22	Free-Energy Barriers and Reaction Mechanisms for the Electrochemical Reduction of CO on the Cu(100) Surface, Including Multiple Layers of Explicit Solvent at pH 0. Journal of Physical Chemistry Letters, 2015, 6, 4767-4773.	4.6	206
23	Layer-by-Layer Degradation of Methylammonium Lead Tri-iodide Perovskite Microplates. Joule, 2017, 1, 548-562.	24.0	199
24	Selective photoelectrochemical oxidation of glycerol to high value-added dihydroxyacetone. Nature Communications, 2019, 10, 1779.	12.8	185
25	Pressureâ€Dependent Polymorphism and Bandâ€Gap Tuning of Methylammonium Lead Iodide Perovskite. Angewandte Chemie - International Edition, 2016, 55, 6540-6544.	13.8	157
26	Constructing High-Loading Single-Atom/Cluster Catalysts via an Electrochemical Potential Window Strategy. Journal of the American Chemical Society, 2020, 142, 3375-3383.	13.7	147
27	Nature of the Active Sites for CO Reduction on Copper Nanoparticles; Suggestions for Optimizing Performance. Journal of the American Chemical Society, 2017, 139, 11642-11645.	13.7	146
28	Constructing FeN4/graphitic nitrogen atomic interface for high-efficiency electrochemical CO2 reduction over a broad potential window. CheM, 2021, 7, 1297-1307.	11.7	133
29	Pd ₂ @Sn ₁₈ ⁴⁻ :  Fusion of Two Endohedral Stannaspherenes. Journal of the American Chemical Society, 2007, 129, 9560-9561.	13.7	116
30	Highly active enzyme–metal nanohybrids synthesized in protein–polymer conjugates. Nature Catalysis, 2019, 2, 718-725.	34.4	115
31	Selective Extraction of C ₇₀ by a Tetragonal Prismatic Porphyrin Cage. Journal of the American Chemical Society, 2018, 140, 13835-13842.	13.7	105
32	Initial Steps of Thermal Decomposition of Dihydroxylammonium 5,5′-bistetrazole-1,1′-diolate Crystals from Quantum Mechanics. Journal of Physical Chemistry C, 2014, 118, 27175-27181.	3.1	101
33	Two-Dimensional Halide Perovskites: Tuning Electronic Activities of Defects. Nano Letters, 2016, 16, 3335-3340.	9.1	94
34	Tuning the Spin Density of Cobalt Single-Atom Catalysts for Efficient Oxygen Evolution. ACS Nano, 2021, 15, 7105-7113.	14.6	90
35	Distinct Crystalâ€Facetâ€Dependent Behaviors for Singleâ€Atom Palladiumâ€On eria Catalysts: Enhanced Stabilization and Catalytic Properties. Advanced Materials, 2022, 34, e2107721.	21.0	78
36	Few-Atom Pt Ensembles Enable Efficient Catalytic Cyclohexane Dehydrogenation for Hydrogen Production. Journal of the American Chemical Society, 2022, 144, 3535-3542.	13.7	72

#	Article	IF	CITATIONS
37	The Key Role of Support Surface Hydrogenation in the CH ₄ to CH ₃ OH Selective Oxidation by a ZrO ₂ -Supported Single-Atom Catalyst. ACS Catalysis, 2019, 9, 8903-8909.	11.2	65
38	Dramatic differences in carbon dioxide adsorption and initial steps of reduction between silver and copper. Nature Communications, 2019, 10, 1875.	12.8	63
39	Edgeâ€Exposed Molybdenum Disulfide with Nâ€Đoped Carbon Hybridization: A Hierarchical Hollow Electrocatalyst for Carbon Dioxide Reduction. Advanced Energy Materials, 2019, 9, 1900072.	19.5	62
40	PdAg bimetallic electrocatalyst for highly selective reduction of CO2 with low COOH* formation energy and facile CO desorption. Nano Research, 2019, 12, 2866-2871.	10.4	61
41	Pb-Activated Amine-Assisted Photocatalytic Hydrogen Evolution Reaction on Organic–Inorganic Perovskites. Journal of the American Chemical Society, 2018, 140, 1994-1997.	13.7	59
42	Two-Dimensional SnO ₂ Nanosheets for Efficient Carbon Dioxide Electroreduction to Formate. ACS Sustainable Chemistry and Engineering, 2020, 8, 4975-4982.	6.7	59
43	Extending Cycle Life of Mg/S Battery by Activation of Mg Anode/Electrolyte Interface through an LiClâ€Assisted MgCl ₂ Solubilization Mechanism. Advanced Functional Materials, 2020, 30, 1909370.	14.9	49
44	Unravelling the Enigma of Nonoxidative Conversion of Methane on Iron Singleâ€Atom Catalysts. Angewandte Chemie - International Edition, 2020, 59, 18586-18590.	13.8	44
45	Mechanism and kinetics of the electrocatalytic reaction responsible for the high cost of hydrogen fuel cells. Physical Chemistry Chemical Physics, 2017, 19, 2666-2673.	2.8	43
46	Predicted Structures of the Active Sites Responsible for the Improved Reduction of Carbon Dioxide by Gold Nanoparticles. Journal of Physical Chemistry Letters, 2017, 8, 3317-3320.	4.6	43
47	Câ^'C Coupling Is Unlikely to Be the Rateâ€Đetermining Step in the Formation of C ₂₊ Products in the Copperâ€Catalyzed Electrochemical Reduction of CO. Angewandte Chemie - International Edition, 2022, 61, .	13.8	43
48	Intramolecular Energy and Electron Transfer within a Diazaperopyrenium-Based Cyclophane. Journal of the American Chemical Society, 2017, 139, 4107-4116.	13.7	42
49	Insights into the Interfacial Lewis Acid–Base Pairs in CeO ₂ â€Loaded CoS ₂ Electrocatalysts for Alkaline Hydrogen Evolution. Small, 2021, 17, e2103018.	10.0	41
50	Theoretical Investigations of Geometry, Electronic Structure and Stability of UO ₆ : Octahedral Uranium Hexoxide and Its Isomers ^{â€} . Journal of Physical Chemistry A, 2010, 114, 8837-8844.	2.5	39
51	Size-Matched Radical Multivalency. Journal of the American Chemical Society, 2017, 139, 3986-3998.	13.7	39
52	Mechanistic Investigations on Thermal Hydrogenation of CO ₂ to Methanol by Nanostructured CeO ₂ (100): The Crystal-Plane Effect on Catalytic Reactivity. Journal of Physical Chemistry C, 2019, 123, 11763-11771.	3.1	35
53	Engineering Ultrafine NiFeâ€LDH into Selfâ€Supporting Nanosheets: Separationâ€andâ€Reunion Strategy to Expose Additional Edge Sites for Oxygen Evolution. Small, 2021, 17, e2103785.	10.0	35
54	Facet engineering in metal organic frameworks to improve their electrochemical activity for water oxidation. Chemical Communications, 2020, 56, 4316-4319.	4.1	32

#	Article	IF	CITATIONS
55	Influence of Constitution and Charge on Radical Pairing Interactions in Tris-radical Tricationic Complexes. Journal of the American Chemical Society, 2016, 138, 8288-8300.	13.7	29
56	The Oxygen Reduction Reaction on Graphene from Quantum Mechanics: Comparing Armchair and Zigzag Carbon Edges. Journal of Physical Chemistry C, 2017, 121, 24408-24417.	3.1	29
57	Artificial Intelligence and QM/MM with a Polarizable Reactive Force Field for Next-Generation Electrocatalysts. Matter, 2021, 4, 195-216.	10.0	29
58	Doping Ruthenium into Metal Matrix for Promoted pHâ€Universal Hydrogen Evolution. Advanced Science, 2022, 9, e2200010.	11.2	29
59	Nonadiabatic Study of Dynamic Electronic Effects during Brittle Fracture of Silicon. Physical Review Letters, 2012, 108, 045501.	7.8	28
60	p-Type Co Interstitial Defects in Thermoelectric Skutterudite CoSb ₃ Due to the Breakage of Sb ₄ -Rings. Chemistry of Materials, 2016, 28, 2172-2179.	6.7	28
61	Selective hydrogenation of acetylene on graphene-supported non-noble metal single-atom catalysts. Science China Materials, 2020, 63, 1741-1749.	6.3	28
62	Boosting the ORR performance of modified carbon black <i>via</i> C–O bonds. Chemical Science, 2019, 10, 2118-2123.	7.4	26
63	Computational Prediction of Graphdiyne-Supported Three-Atom Single-Cluster Catalysts. CCS Chemistry, 2023, 5, 152-163.	7.8	25
64	Pressureâ€Dependent Polymorphism and Bandâ€Gap Tuning of Methylammonium Lead Iodide Perovskite. Angewandte Chemie, 2016, 128, 6650-6654.	2.0	24
65	<i>In Situ</i> Precise Tuning of Bimetallic Electronic Effect for Boosting Oxygen Reduction Catalysis. Nano Letters, 2021, 21, 7753-7760.	9.1	24
66	Dependence on the structure and surface polarity of ZnS photocatalytic activities of water splitting: first-principles calculations. Physical Chemistry Chemical Physics, 2013, 15, 9531.	2.8	23
67	Efficient Nitrogen Fixation via a Redox-Flexible Single-Iron Site with Reverse-Dative Iron → Boron σ Bonding. Journal of Physical Chemistry A, 2018, 122, 4530-4537.	2.5	23
68	RuO2 clusters derived from bulk SrRuO3: Robust catalyst for oxygen evolution reaction in acid. Nano Research, 2022, 15, 1959-1965.	10.4	23
69	A polyoxometalate cluster-based single-atom catalyst for NH ₃ synthesis <i>via</i> an enzymatic mechanism. Journal of Materials Chemistry A, 2022, 10, 6165-6177.	10.3	23
70	Manganese vacancy-confined single-atom Ag in cryptomelane nanorods for efficient Wacker oxidation of styrene derivatives. Chemical Science, 2021, 12, 6099-6106.	7.4	22
71	Predicted roles of defects on band offsets and energetics at CIGS (Cu(In,Ga)Se2/CdS) solar cell interfaces and implications for improving performance. Journal of Chemical Physics, 2014, 141, 094701.	3.0	20
72	The df–d Dative Bonding in a Uranium–Cobalt Heterobimetallic Complex for Efficient Nitrogen Fixation. Inorganic Chemistry, 2019, 58, 7433-7439.	4.0	19

#	Article	IF	CITATIONS
73	Chemical design and synthesis of superior single-atom electrocatalysts <i>via in situ</i> polymerization. Journal of Materials Chemistry A, 2020, 8, 17683-17690.	10.3	19
74	Synergy between a Silver–Copper Surface Alloy Composition and Carbon Dioxide Adsorption and Activation. ACS Applied Materials & Interfaces, 2020, 12, 25374-25382.	8.0	19
75	N 2 Reduction on Feâ€Based Complexes with Different Supporting Mainâ€Group Elements: Critical Roles of Anchor and Peripheral Ligands. Small Methods, 2019, 3, 1800340.	8.6	17
76	Tuning radical interactions in trisradical tricationic complexes by varying host-cavity sizes. Chemical Science, 2020, 11, 107-112.	7.4	14
77	Suppression of surface recombination in CuInSe2 (CIS) thin films via Trioctylphosphine Sulfide (TOP:S) surface passivation. Acta Materialia, 2016, 106, 171-181.	7.9	13
78	Unravelling the Enigma of Nonoxidative Conversion of Methane on Iron Singleâ€Atom Catalysts. Angewandte Chemie, 2020, 132, 18745-18749.	2.0	12
79	Two-dimensional Zr/Hf-hydroxamate metal–organic frameworks. Chemical Communications, 2022, 58, 3601-3604.	4.1	12
80	The Key Role of Competition between Orbital and Electrostatic Interactions in the Adsorption on Transition Metal Singleâ€Atom Catalysts Anchored by Nâ€doped Graphene. ChemCatChem, 2022, 14, .	3.7	12
81	Formation of the –N(NO)N(NO)– polymer at high pressure and stabilization at ambient conditions. Proceedings of the National Academy of Sciences of the United States of America, 2013, 110, 5321-5325.	7.1	10
82	Non-adiabatic dynamics modeling framework for materials in extreme conditions. Mechanics of Materials, 2015, 90, 243-252.	3.2	10
83	Manipulating Stabilities and Catalytic Properties of Trinuclear Metal Clusters through Tuning the Chemical Bonding: H ₂ Adsorption and Activation. Journal of Physical Chemistry C, 2017, 121, 10992-11001.	3.1	10
84	Theoretical investigation on hydrogenation of dinitrogen triggered by singly dispersed bimetallic sites. Journal of Materials Chemistry A, 2022, 10, 6146-6152.	10.3	10
85	Deformation Induced Solid–Solid Phase Transitions in Gamma Boron. Chemistry of Materials, 2014, 26, 4289-4298.	6.7	9
86	Breaking the scaling relations for efficient N2-to-NH3 conversion by a bowl active site design: Insight from LaRuSi and isostructural electrides. Chinese Journal of Catalysis, 2022, 43, 2183-2192.	14.0	9
87	A rational design of an efficient counter electrode with the Co/Co ₁ P ₁ N ₃ atomic interface for promoting catalytic performance. Materials Chemistry Frontiers, 2021, 5, 3085-3092.	5.9	8
88	Singly Dispersed Bimetallic Sites as Stable and Efficient Single-Cluster Catalysts for Activating N ₂ and CO ₂ . Journal of Physical Chemistry C, 2021, 125, 27192-27198.	3.1	8
89	Stability of NNO and NPO Nanotube Crystals. Journal of Physical Chemistry Letters, 2014, 5, 485-489.	4.6	6
90	In Silico Optimization of Organic–Inorganic Hybrid Perovskites for Photocatalytic Hydrogen Evolution Reaction in Acidic Solution. Journal of Physical Chemistry C, 2018, 122, 20918-20922.	3.1	6

#	Article	IF	CITATIONS
91	Câ^'C Coupling Is Unlikely to Be the Rateâ€Determining Step in the Formation of C ₂₊ Products in the Copperâ€Catalyzed Electrochemical Reduction of CO. Angewandte Chemie, 2022, 134, .	2.0	6